Unveiling the Sulfur–Sulfur Bridge: Accurate Structural and Energetic Characterization of a Homochalcogen Intermolecular Bond

COMMUNICATION

On the way to the sulfur-sulfur bridge: accurate structural and energetic characterization of a homo chalcogen inter-molecular bond

Daniel A. Obenchain,[a],† Lorenzo Spada,[b,c],† Silvia Alessandrini,[c] Sergio Rampino,[c] Sven Herbers,[a] Nicola Tasinato,[c] Marco Mendolicchio,[c] Peter Kraus,[a] Jürgen Gauss,[d] Cristina Puzzarini,[b] Jens-Uwe Grabow,[a],* Vincenzo Barone[c],*

Abstract: By combining rotational spectroscopy in supersonic expansion with the capability of state-of-the-art quantum-chemical computations in accurately determining structural and energetic properties, the genuine nature of a sulfur-sulfur chalcogen bond between dimethyl sulfide and sulfur dioxide has been unveiled in a gas-jet environment free from collision, solvent and matrix perturbations. A SAPT analysis pointed out that electrostatic S···S interactions play the dominant role in determining the stability of the complex, largely overcoming dispersion and C-H···O hydrogen-bond contributions. Indeed, in agreement with the analysis of the quadrupole-coupling constants and of the methyl internal rotation barrier, the NBO and NOCV/CD approaches show a marked charge transfer between the sulfur atoms. Based on the assignment of the rotational spectra for 7 isotopologues, an accurate semi-experimental equilibrium structure for the heavy-atom backbone of the molecular complex has been determined, which is characterized by a S···S distance (2.947(3) Å) well below the sum of van der Waals radii.

Among chemical elements, sulfur is widespread in nature, and in particular in biologically active natural products,[1] where it strongly affects molecular recognition mechanisms.[1,2] As a consequence, the effect of substitution of oxygen by sulfur on many properties is of particular relevance in biochemistry[3] and chemical reactivity.[4] Therefore, the investigation of the changes occurring in structural,[5] chemical-physical[6] and spectroscopic properties[7] upon such substitution is of much general interest.

In parallel, non-covalent chalcogen-bond interactions have attracted much attention because of the fundamental role they play in different fields such as catalysis,[8] drug design,[1] self-assembly processes,[9] and crystal packing.[10] Understanding the mechanisms at the basis of these technological processes requires the characterization of the directionality, strength, and nature of such interactions[11] as well as a comprehensive analysis of their competition with other non-covalent bonds, also taking into account the tuning of these properties by different environments. In this respect, in analogy to the halogen bond[12] the sulfur atom can act either as a chalcogen bond donor (due to a σ-[13,14] or π-hole[13,15] on sulfur) or as acceptor (because of a lone-pair on sulfur, as in thioethers[14]).

To summarize, the variety of sulfur compounds found in nature as well as the dual role that sulfur can play, call for a comprehensive analysis and characterization of the sulfur···sulfur noncovalent chalcogen interactions. A step forward in this direction requires, in addition to the elucidation of the contributions stabilizing the interaction, the accurate knowledge of the structural parameters involved in such linkage. Dimethyl sulfide (DMS) is a good candidate because the lack of SH bonds avoids any competition between putative chalcogen and hydrogen bonds nearby the same sulfur atom. At the same time, the negatively charged sulfur atom of DMS should lead to a stabilizing electrostatic interaction with the strongly positive sulfur atom of sulfur dioxide (SO_2). The DMS-SO_2 complex has thus been studied by combining rotational spectroscopy in supersonic expansion and state-of-art quantum-chemical (QC) calculations, thus relying on their capability to unveil the genuine nature of non-covalent interactions in an environment free from solvation, matrix and crystal-packing effects.

As a starting point, a full geometry optimization was performed by means of the so-called “cheap” composite scheme defined in ref. [16], in which the CCSD(T)/cc-pVTZ[17,18] geometrical parameters are improved by means of an extrapolation to the complete basis set (CBS) limit and by the inclusion of the core-valence (CV) contribution, both at the MP2 level.[19] This optimized geometry (hereafter referred to as “cheap”) straightforwardly provided the equilibrium rotational constants (B_e), which were then corrected for vibrational effects[20] obtained at the B2PLYP-D3/maug-cc-pVTZ-*d*H level[21,22] in order to obtain the vibrational ground-state rotational constants (B_0, see Table 1). The B2PLYP-D3/maug-cc-pVTZ-*d*H cubic and semi-diagonal quartic constants were also used to derive the centrifugal-distortion parameters by means of Watson *S*-reduced Hamiltonian[23] in the framework of second-order vibrational perturbation theory (VPT2).[24] A full account of the computational details together with the corresponding results is given in the Supporting Information (SI).

Guided by quantum-chemical calculations, the rotational spectrum of the main isotopic species of the DMS-SO_2 complex was recorded, as detailed in the *Experimental Section*, and assigned. The combination of experimental data for the most

[a] Dr. D. A. Obenchain, Mr. S, Herbers, Dr. P. Kraus, Prof. Dr. J.U. Grabow
Institut für Physikalische Chemie und Elektrochemie,
Leibniz Universität Hannover,
Callinstraße 3A, 30167 Hannover, Germany
E-mail: jens-uwe.grabow@pci.uni-hannover.de
[b] Dr. L. Spada, Prof. Dr. C. Puzzarini
Dipartimento di Chimica “Giacomo Ciamician,”
”Università di Bologna,
Via Selmi 2, I-40126, Bologna, Italy
[c] Dr. L. Spada, Ms. S. Alessandrini, Dr. S. Rampino, Dr. N. Tasinato, Mr. M. Mendolicchio, Prof. Dr. V. Barone
Scuola Normale Superiore
Piazza dei Cavalieri 7, I-56126, Pisa, Italy
E-mail: vincenzo.barone@sns.it
[d] Prof. Dr. J. Gauss
Institut für Physikalische Chemie,
Johannes Gutenberg-Universität Mainz,
Duesbergweg 10-14, 55128 Mainz, Germany
[†] These authors equally contributed to this work.

Supporting information for this article is given via a link at the end of the document.

abundant isotopologue species and the accurate quantum-chemical predictions led to minimal amounts of searching on the narrow-bandwidth spectrometer, and to the detection of 7 isotopologues (i.e., the parent species, and the singly substituted ^{34}S, ^{33}S, ^{13}C, ^{18}O isotopologues) in natural abundance. Fits of the observed transitions (detailed lists, for each isotopologue, are given in Tables S1-S7 of the SI) were carried out using the XIAM[25] program within the *I*^{r} representation of Watson's *S* reduction. The XIAM program was chosen for its capability to fit the methyl internal rotation coupling and, if a quadrupolar nucleus is present (as in the case of single ^{33}S-substituted species), the nuclear hyperfine splitting (an example is shown in Figure 1 for the $^{33}SO_2\cdots$DMS species). This arises from the interaction of the non-spherical nuclear charge distribution (^{33}S nuclear spin, I = 3/2) with a nonzero electric field gradient at the nucleus, and the corresponding hyperfine components are labeled using the quantum number resulting from the *F=I+J* coupling scheme.

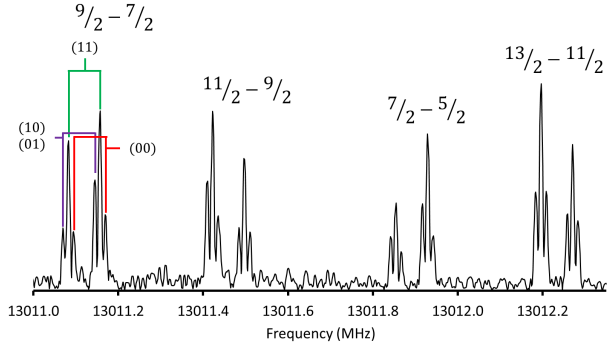

Figure 1. Combination of several spectra collected on the COBRA instrument for the $5_{05} - 4_{04}$ transition of the $^{33}SO_2\cdots$DMS isotopologue. Each transition is split into a Doppler pair arising from the coaxial arrangement of the jet and resonator. The three closely spaced transitions are the internal rotation components labelled in the lowest frequency set (See ref. [26] for labels). Each of the four sets represents a different *F'*-*F*" component of the nuclear quadrupole hyperfine pattern.

While a full account of the spectroscopic parameters resulting from the fits is provided in the SI, Table 1 collects the computed (only for the main isotopologue) and experimental rotational constants. The comparison between the calculated and experimentally derived rotational constants points out a good agreement with deviations well within 0.5%, thus demonstrating the important role played by accurate QC computations in guiding the recording and analysis of the rotational spectrum.

Table 1. Rotational constants[a] of the $SO_2\cdots S(CH_3)_2$ isotopologues.

	A (MHz)	*B* (MHz)	*C* (MHz)
$SO_2\cdots S(CH_3)_2$	3478.40[b]	1504.90[b]	1219.79[b]
	3490.1920(16)	1497.76387(44)	1216.39695(35)
$^{34}SO_2\cdots S(CH_3)_2$	3484.0255(41)	1477.70534(28)	1203.85113(20)
$SO_2\cdots ^{34}S(CH_3)_2$	3473.9912(39)	1475.64069(27)	1203.70117(19)
$SO_2\cdots ^{33}S(CH_3)_2$	3481.9380(90)	1486.51807(47)	1209.96356(26)
$^{33}SO_2\cdots S(CH_3)_2$	3487.028(10)	1487.57426(31)	1210.03633(20)
$S^{18}O^{16}O\cdots S(CH_3)_2$	3414.9948(81)	1475.98433(27)	1194.47542(27)
$SO_2\cdots S(^{13}CH_3)(^{12}CH_3)$	3438.8559(56)	1484.77801(20)	1203.33928(20)

[a] Numbers in parenthesis are 1σ uncertainties in the least significant digit. [b] Values obtained from theory (see text).

Similarly, computed spectroscopic constants were obtained for the other isotopic species investigated, also including, for the ^{33}S-containing isotopologues, the nuclear quadrupole coupling constants. The corresponding results are found in the SI.

Computations were also extended to the evaluation of the interaction electronic energy, there employing a composite scheme analogous to that used for the structural evaluation, with the only difference in the extrapolation to the CBS limit, which was estimated by a two-step procedure, with the HF-SCF and MP2 correlation energies extrapolated using different formulae[27,28]. The total electronic energy was then corrected for the zero-point energy (ZPE) contribution obtained at the B2PLYP-D3/m-aug-cc-pVTZ-*d*H anharmonic level as well as for the basis-set superposition error (BSSE)[29], thus leading to a final value of 23.5 kJ/mol (a full account is given in the SI).

The investigation of 7 isotopologues opens the way for a semi-experimental (SE) determination of the equilibrium structure. This was obtained by a least-squares fit of the B_0's of the 7 isotopologues corrected by computed vibrational contributions, employing the MSR software[30], with all rotational constants being equally weighted. The lack of data due to the missing information on deuterated species has been overcome by fixing all parameters involving hydrogen atoms to the corresponding computed values. Two different SE equilibrium structures were determined by using fixed constraints for the hydrogen-related geometrical parameters calculated either at the B2PLYP-D3/maug-cc-pVTZ-*d*H (r_e^{SE}(B2PLYP)) or by means of the "cheap" scheme (r_e^{SE}(cheap)). Both calculations were corrected by using B2PLYP-D3/maug-cc-pVTZ-*d*H vibrational corrections and provided very similar structural parameters. In parallel, a vibrationally-averaged structure r_0, was also computed by fitting the experimental ground-state rotational constants without any correction for vibrational effects. In such determination, the fixed parameters were evaluated by means of two different strategies. The first one consists in directly using the computed vibrationally-averaged B2PLYP-D3/maug-cc-pVTZ-*d*H values (at 0 K, r_0^{B2PLYP}), while the second determination exploits for them the r_0^{hyb}= r_e^{cheap}+ (r_0^{B2PLYP}-r_e^{B2PLYP}) hybrid approach, where r_e^{cheap} and r_e^{B2PLYP} are the "cheap" and B2PLYP-D3/maug-cc-pVTZ-*d*H equilibrium values, respectively. A selection of structural parameters is given in Figure 2, there comparing r_e(cheap) to r_e^{SE}(cheap) and r_0, where for the latter a generic r_0 is provided because the two strategies mentioned above led to very similar results (see SI).

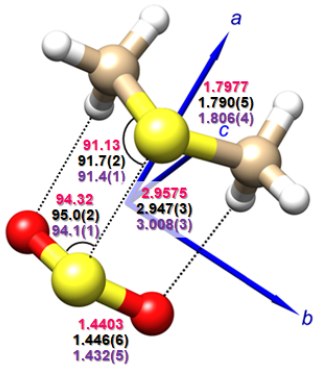

Figure 2. The DMS-SO_2 complex: selected structural parameters (bond distances in Å and angles in degrees). Computed r_e(cheap) in pink, r_e^{SE} (cheap) in black, and vibrationally-averaged r_0 in violet. The principal inertia axes are also shown.

The role played by different interactions in determining the overall stability of the observed adduct has been investigated by means of well-established models. The nature of the inter-molecular interaction has been unraveled using the symmetry adapted perturbation theory (SAPT),[31] at the SAPT2+(CCD)dMP2 level in conjunction with the aug-cc-pVTZ basis set. The results show that the electrostatic interaction is by far the largest contribution, while dispersion and induction are comparable in magnitude, and altogether are larger than the exchange contribution (see SI for details), with the overall binding energy (-30.74 kJ/mol + zero point correction) in a good agreement with the "cheap" value ($E_{B(equilibrium)}$= -30.00 kJ/mol, $E_{B(equilbrium+ZPE)}$ = -24.95 kJ/mol, $E_{B(equilbrium+ZPE+BSSE)}$= -23.46 kJ/mol).

A detailed analysis of the electron charge rearrangement occurring upon binding of DMS to SO_2 has been carried out by means of the so-called Natural Orbital for Chemical Valence/Charge-Displacement (NOCV/CD) scheme.[32] In the NOCV/CD framework, the overall charge rearrangement $\Delta\rho'(x,y,z)$ (whose formal definition is given in the SI) can be decomposed into a weighed sum of a few important, chemically meaningful components, $\Delta\rho'_k$. A suitable integration of these terms (see SI for details) returns a charge-flow profile $\Delta q(z)$, providing, for each point z along the interaction axis, the amount of electron charge that, upon bond formation, has flown from right to left across a plane orthogonal to the z-axis through that point. The overall $\Delta\rho'(x,y,z)$ resulting from the binding of DMS to SO_2 (see Figure S11.1 of the SI) shows that the most involved atoms in the charge rearrangement are the S-S couple and the two H-O pairs possibly engaged in two hydrogen bonds. Focusing on the S-S couple, charge accumulation is observed in the region amid the atoms suggesting electron sharing as a component part of their interaction. As fully detailed in the SI, the overall charge rearrangement is almost entirely recovered by the first and most important component ($\Delta\rho'_1$), which mainly involves the charge flow between the two sulfur atoms (DMS→SO_2, see blue curve in Figure 3), and whose contribution is about six times larger than others. The charge-flow profile $\Delta q(z)$ along the interaction axis z associated with the overall $\Delta\rho'(x,y,z)$ is shown as a black line in Figure 3. By fixing a plausible boundary between the fragments (see the dashed vertical line in Figure 3 and SI for explanation), a net charge transfer of 0.12 e from DMS to SO_2 is obtained.

In weakly bound and van der Waals complexes, only small changes in electric nuclear quadrupole coupling constants are expected with respect to the separated fragments. Using the r_e^{SE}(cheap) geometry, the ^{33}S quadrupole coupling tensor of each individual molecule is rotated into the axis system of the complex. The experimental value of the component along the S-S axis, χ_{aa}, is 16.88% more negative in the $SO_2\cdots(CH_3)_2{}^{33}S$ complex than in the $(CH_3)_2{}^{33}S$[33] monomer, while the $^{33}SO_2\cdots(CH_3)_2S$ component is 6.13% more positive than that in the $^{33}SO_2$ monomer.[34] This observation is a further strong evidence in support of the predicted non-negligible charge transfer from DMS to SO_2. Another spectroscopic evidence of the strong interaction between the two sulfur atoms can be found in the change of the measured internal rotation potential V_3. In free DMS, the V_3 barrier was found to be 735.784(44) cm^{-1}.[35] Only a small barrier change is observed in the Ar complex with DMS[36], 736.17(32) cm^{-1}, suggesting a relatively small interaction between the rare gas atom and sulfur. In the complex with carbon monoxide,[37] the barrier increases to 745.5 (30) cm^{-1}, whereas a significant decrease (to 656.1(14) cm^{-1}) is noted in the complex with SO_2. Since an interaction between the oxygen atoms of SO_2 and the methyl tops would likely raise the barrier, the observed decrease has to come from an electron density depletion on the sulfur of DMS, this consideration being again in agreement with a charge transfer from the DMS to the SO_2 sulfur.

A Natural Bond Orbital (NBO) analysis[38] (see SI for full details), shows that at the 2nd order of perturbation the largest contribution to the stabilization of the complex is due to the interaction between the S lone pair of DMS and the S-O antibonding orbital of SO_2. Furthermore, NBO charges point out a large charge transfer flowing from sulfur in DMS, through sulfur in SO_2, to the oxygen atoms, which increase their negative charges (see Table S13.2). These results are in full agreement with the other analyses, thus providing a further confirmation of the previous observations.

The r(S-S) bond length also provides insights on the interaction between the sulfur atoms. From the r_e^{SE}(cheap) structure, the r(S-S) of 2.947(3) Å found in the complex is 0.63 Å shorter than the sum of the van der Waals radii.[39] This difference is significantly larger than that observed for the $(CH_3)_2O\cdots SO_2$[40] complex, for which the measured r(S-O) of 2.884(2) Å is 0.44 Å shorter than the vdW radii.

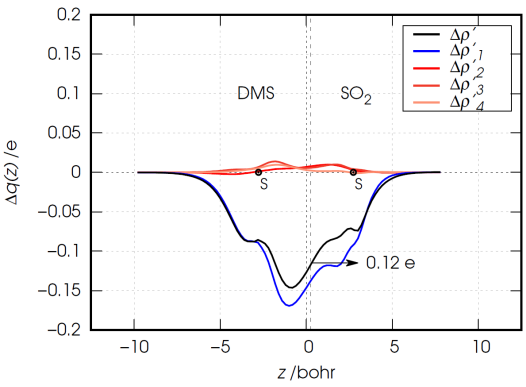

Figure 3. Charge-flow profile Δq(z) along the interaction z axis associated with density differences $\Delta\rho'$ and $\Delta\rho'_k$ (k = 1, 2, 3, 4) due to the interaction between DMS and SO_2.

A pseudo diatomic approximation is often employed to estimate the stabilization energy of typical van der Waals complexes.[41] The model requires that the straight-line joining the centers-of-mass of the two partners in the complex is nearly parallel to the a-axis, as is actually the case for the DMS-SO_2 adduct. The approach is based on the estimation of the following force constant:

$$k_s = \frac{16\pi^4\mu^2 R_{cm}^2\left[3B^4+3C^4+2B^2C^2\right]}{hD_J} \qquad (1)$$

where μ is the reduced mass, R_{cm} is the center of mass distance between the two monomers, B and C are the rotational constants, and D_J is a centrifugal distortion constant. Here, the R_{cm} value is taken from the r_e^{SE}(cheap) structure. The pseudo diatomic model then employs a Leonard-Jones potential to determine the binding energy of the complex, E_B:

$$E_B = \frac{1}{72}k_s R_{cm}^2 \qquad (2)$$

This gives a result of E_B = -43.6(6) kJ/mol, which significantly differs from the value predicted by the “cheap” scheme (see above) of -23.5 kJ/mol. As the accuracy of the spectroscopic constants and the r_e^{SE} structure obtained by the “cheap” model

are largely documented, we must conclude that a simple Leonard-Jones potential is not able to describe the binding of DMS and SO_2, the reason likely being related to the presence of other low frequency modes, as fully discussed in the SI.

In summary, in the gas phase complex between DMS and SO_2 a sulfur-sulfur noncovalent interaction has been unveiled, which largely prevails over the C-H···O hydrogen bonds. Both the NBO and NOCV/CD approaches point out a marked charge transfer involving the sulfur atoms, also confirmed by the ^{33}S quadrupole coupling constant analysis. The electrostatic contribution to the S-S interaction plays a dominant role in stabilizing the molecular adduct according to a SAPT analysis. The computed binding energy value points out that the strength of the sulfur-sulfur interaction is similar to that typical in neutral hydrogen bonds. A not less important result of the present study is the accurate structural characterization of the DMS-SO_2 complex. This relies on the semi-experimental equilibrium structure approach, applied for the first time to a molecular complex, which combines computed vibrational corrections with the experimentally determined rotational constants of seven isotopologues. It is noteworthy that the semi-experimental equilibrium structure is very close to its purely theoretical counterpart based on the "cheap" composite approach.

Experimental Section

The complex is formed in a rotationally cold (less than 4 K), supersonic jet that is expanded from a mixture of 1.4-2.0% dimethyl sulfide, 1.0-1.3% SO_2 in Ar (99.999% purity) at stagnation pressure of 1 bar. Initial measurements were made using the broadband IMPACT (In-phase/quadrature-phase-Modulation Passage-Acquired-Coherence technique) spectrometer[42] between 7-16 GHz. Further measurements were made using the COBRA (Coaxially Aligned Beam Resonator Arrangement) Fourier Transform Microwave spectrometer[43], which prolongs the observation time compared to a Fabry-Perot type cavity setup used in the style of Balle and Flygare[44] to record molecular signals, primarily rotational transitions.

Acknowledgements

The authors acknowledge the Alexander von Humboldt Foundation, the Land Niedersachsen, and the DFG for financial support, and W. B. Garden for helpful discussions. This work has also been supported by MIUR "PRIN 2015" funds (Grant Number 2015F59J3R), by the University of Bologna (RFO funds), and by Scuola Normale Superiore (Grant Number SNS18_B_TASINATO). The SMART@SNS Laboratory (http://smart.sns.it) is acknowledged for providing high-performance computer facilities. The authors also acknowledge Mr. Alessio Melli for the graphical abstract preparation.

Keywords: semi-experimental equilibrium structure • rotational spectroscopy • quantum chemistry • bond analysis • energy and charge decomposition models

[1] B. R. Beno, K.-S. Yeung, M. D. Bartberger, L. D. Pennington, N. A. Meanwell, *J. Med. Chem*. **2015**, *58*, 4383−4438.
[2] R. J. Fick, G. M. Kroner, B. Nepal, R. Magnani, S. Horowitz, R. L. Houtz, S. Scheiner, R.C. Trievel, *ACS Chem. Biol*. **2016**, *11*, 748–754.
[3] P. Thaplyal, A. Ganguly, B. L. Golden, S. Hammes-Schiffer, P. C. Bevilacqua, *Biochemistry* **2013**, 52, 6499–6514.
[4] B. A. Gregersen, X. Lopez, D. M. York, *J. Am. Chem. Soc*. **2003**, *125*, 7178-7179.
[5] E. Penocchio, M. Mendolicchio, N. Tasinato, V. Barone, *Can. J. Chem*. **2016**, *94*, 1065–1076.
[6] M.-K. Han, Y.-S. Jin, B. Kyu Yu, W. Choi, T.-S. Youb, S.-J. Kim, *J. Mater. Chem. A* **2016**, *4*, 13859–13865.
[7] C. Falantin, A. Moncomble, A. Le Person, J.-P. Cornard, *Spectrochim. Acta A* **2017**, *187*, 49–60 and references therein.
[8] S. Benz, J. López-Andarias, J. Mareda, N. Sakai, S. Matile, *Angew. Chem. Int. Ed.* **2017**, *56*, 812 –815.
[9] a) L. Chen, J. Xiang, Y. Zhao, Q. Yan, *J. Am. Chem. Soc*. **2018**, *140*, 7079−7082; b) R. Gleiter, G. Haberhauer, D. B. Werz, F. Rominger, C. Bleiholder, *Chem. Rev*. **2018**, *118*, 2010-2041.
[10] J. Fanfrlík, Adam Přáda, Z. Padělková A. Pecina, J. Macháček, M. Lepšík, J. Holub, Aleš Růžička, D. Hnyk, P. Hobza, *Angew. Chem. Int. Ed.* **2014**, *53*, 10139 –10142.
[11] a) D. J. Pascoe, K. B. Ling, S. L. Cockroft, *J. Am. Chem. Soc*. **2017**, *139*, 15160−15167; b) U. Adhikari, S. Scheiner, *Chem. Phys. Lett*. **2012**, *532*, 31–35; c) W. Wang, B. Ji, Y. Zhang, *J. Phys. Chem. A* **2009**, *113*, 8132–8135; d) M. H. Kolář, P. Hobza, *Chem. Rev*. **2016**, *116*, 5155−5187; e) A. Bauzá, T. J. Mooibroek, A. Frontera, *ChemPhysChem* **2015**, *16*, 2496 –2517.
[12] G. R. Desiraju, P. S. Ho, L. Kloo, A. C. Legon, R. Marquardt, P. Metrangolo, P. Politzer, G. Resnati, K. Rissanen, *Pure Appl. Chem.* **2013**, *85*, 1711–1713.
[13] P. Politzer, J. S. Murray, *J. Comput. Chem*. **2018**, *39*, 464–471.
[14] Y. Geboes, E. De Vos, W. A. Herrebout, *New J. Chem*. **2018**, *42*, 10563-10571.
[15] A. C. Legon, *Phys. Chem. Chem. Phys.*, **2017**, *19*, 14884--14896.
[16] C. Puzzarini, V. Barone, *Phys. Chem. Chem. Phys*. **2011**, *13*, 7158-7166.
[17] a) G.D. Purvis III, R.J. Bartlett, *J. Chem. Phys.* **1982**, *76*, 1910-1918; b) K. Raghavachari, G.W. Trucks, J.A. Pople, M. Head-Gordon, *Chem. Phys. Lett*. **1989**, *157*, 479-483.
[18] a) T.H. Dunning Jr., *J. Chem. Phys.* **1989**, *90*, 1007-1023. b) D.E. Woon, T.H. Dunning Jr, *J. Chem. Phys*. **1993**, *98*, 1358.
[19] C. Møller, M.S. Plesset, *Phys. Rev*. **1934**, *46*, 618-622.
[20] D. Papoušek, M. R. Aliev, *Molecular Vibrational–Rotational Spectra*, Elsevier, Amsterdam, **1982**.
[21] a) S. Grimme, *J. Chem. Phys*. **2006**, *124*, 034108; b) S. Grimme, J. Antony, S. Ehrlich, H. Krieg, *J. Chem. Phys*. **2010**, *132*, 154104.
[22] a) E. Papajak, H. R. Leverentz, J. Zheng, D. G. Truhlar, *J. Chem. Theory Comput*. **2009**, *5*, 1197-1202. b) T. Fornaro, M. Biczysko, J. Bloino, V. Barone, *Phys. Chem. Chem. Phys*. **2016**, *18*, 8479-8490.
[23] J. K. G. Watson in *Vibrational Spectra and Structure*, Vol. 6, Ed. J.R. Durig, Elvisier, New York, Amsterdam **1977**.
[24] I. M. Mills in *Molecular Spectroscopy: Modern Research*, Eds. K. N. Rao and C.W. Mathews, Academic Press, New York **1972**.
[25] H. Hartwig, H. Dreizler, *Z. Naturforsch* **1996**, *51a*, 923-932.
[26] V. Van, W. Stahl, H. V. L. Nguyen, *Phys. Chem. Chem. Phys*. **2015**, *17*, 32111—32114.
[27] D. Feller, *J. Chem. Phys*. **1993**, *98*, 7059-7071.
[28] T. Helgaker, W. Klopper, H. Koch, J. Noga, *J. Chem. Phys*. **1997**, *106*, 9639-9646.
[29] S. F. Boys, F. Bernardi, *Mol. Phys.* **1970**, *19*, 553-566.
[30] M. Mendolicchio, E. Penocchio, D. Licari, N. Tasinato, V. Barone, *J. Chem. Theory Comput.* **2017**, *13*, 3060-3075.
[31] B. Jeziorski, R. Moszynski, K. Szalewicz, *Chem. Rev*. **1994**, *94*, 1887 – 1930.
[32] a) G. Bistoni, S. Rampino, F. Tarantelli, L. Belpassi, *J. Chem. Phys.* **2015**, *142*, 084112. b) A. Salvadori, M. Fusè, G. Mancini, S. Rampino, V. Barone, *J. Comput. Chem.* **2018**, https://doi.org/10.1002/jcc.25523 c) M. Fusè, I. Rimoldi, G. Facchetti, S. Rampino, V. Barone, *Chem. Comm*. **2018**, *54*, 2397-2400.
[33] U. Kretschmer, H. Hartwig, H. Dreizler, *J. Mol. Spectrosc.* **1995**, *174*, 137-150.
[34] H. S. P. Müller, J. Farhoomand, E. A. Cohen, B. Brupbacher-Gatehouse, M. Schäfer, A. Bauder, G. Winnewisser, *J. Mol. Spectrosc.* **2000**, *201*, 1-8.
[35] A. Jabri, V. Van, H. V. L. Nguyen, H. Mouhib, F. Kwabia Tchana, L. Manceron, W. Stahl, I. Kleiner, *A&A* **2016**, *589*, A127.
[36] Y. Tatamitani, A. Sato, Y. Kawashima, N. Ohashi, J. M. LoBue, E. Hirota, *J. Mol. Spectrosc.* **2009**, *257*, 11-19.
[37] A. Sato, Y. Kawashima, E. Hirota, *J. Mol. Spectrosc.* **2010**, *263*, 135–141.
[38] E. D. Glendening, C. R. Landis, F. Weinhold, *WIREs Comput. Mol. Sci.* **2012**, *2*, 1-42.
[39] M. Mantina, A. C. Chamberlin, R. Valero, C. J. Cramer, D. G. Truhlar, *J. Phys. Chem. A* **2009**, *113*, 5806-5812.
[40] J. J. Oh, K. W. Hillig II, R. L. Kuczkowski, *Inorg. Chem.* **1991**, *30*, 4583-4588.
[41] a) D. J. Millen, *Can. J. Chem*. **1985**, *63*, 1477-1479; b) S. E. Novick, S. J. Harris, K. C. Janda, W. Klemperer, *Can. J. Phys*. **1975**, *53*, 2007-2015.
[42] M. K. Jahn, D. A. Dewald, D. Wachsmuth, J.-U. Grabow, S. C. Mehrotra, *J. Mol. Spectrosc.* **2012**, *280*, 54-60.
[43] J. U. Grabow, W. Stahl, H. Dreizler, *Rev. Sci. Instrum*. **1996**, *67*, 4072-4084.
[44] T. J. Balle, W. H. Flygare, *Rev. Sci. Instrum*. **1981**, *52*, 33-45.

Entry for the Table of Contents (Please choose one layout)

Layout 1:

COMMUNICATION

A sulfur···sulfur noncovalent interaction has been characterized in the dimethyl sulfide – sulfur dioxide adduct by combining rotational spectroscopy in supersonic expansion and state-of-the-art quantum-chemical calculations. A marked charge transfer takes place in the complex, whose stabilization energy is mainly determined by electrostatics with respect to dispersion contributions. The joint experiment-theory investigation also allowed the determination of an accurate semi-experimental equilibrium structure for the heavy atom backbone.

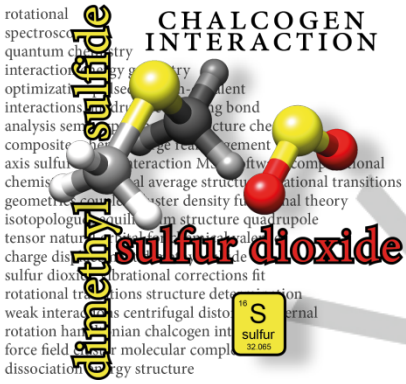

Daniel A. Obenchain, Lorenzo Spada, Silvia Alessandrini, Sergio Rampino, Sven Herbers, Nicola Tasinato, Marco Mendolicchio, Peter Kraus, Jürgen Gauss, Cristina Puzzarini, Jens-Uwe Grabow, Vincenzo Barone**

Page No. – Page No.

On the way to the sulfur-sulfur bridge: accurate structural and energetic characterization of a homo chalcogen inter-molecular bond